Journal of the Serbian Society for Computational Mechanics

http://www.sscm.kg.ac.rs/jsscm/

JSSCM Journal of the Serbian Society for Computational Mechanics
ISSN 1820-6530
e-ISSN 2620-1941
СРПСКО ДРУШТВО ЗА РАЧУНСКУ МЕХАНИКУ
SERBIAN SOCIETY FOR COMPUTATIONAL MECHANICS
СДРМ
http://www.sscm.kg.ac.rs/jsscm

Accepted November 23rd 2022

Thermal analysis of laminar water flow over a backward facing channel with carbon nanoparticles

Sandip Saha[1]. V. Ramachandra Prasad[2*]. O. Anwar Beg[3]

[1]Division of Mathematics, School of Advanced Sciences, Vellore Institute of Technology, Chennai, India

[2*]Division of Mathematics, School of Advanced Sciences, Vellore Institute of Technology, Vellore, India

[3]Department of Aeronautical/Mechanical Engineering, School of Science, Engineering and Environment (SEE), University of Salford, Newton Building, Manchester, M5 4WT, UK

Abstract

In the last few years, the thermo-hydraulic study of nanofluid flow bifurcation phenomena have become a great interest and useful tool in many engineering applications. FVM has been employed in this article to numerically explore the laminar water flow over a backward facing channel with or without carbon nanoparticles (CN). The problem formulated in this paper has been solved by considering the effects of nanoparticle weight percentages ($w\%$), such as 0.00, 0.12, and 0.25 for different Reynolds number (Re). Nusselt number distribution ($Nu(x)$), coefficient of skin friction (C_f), characteristics of pressure drop ($\triangle p$), velocity contours, static temperature, pumping power (P_p) and thermal resistance factor (R) have been investigated to know the behavior of thermo-hydraulic flow bifurcation phenomena. The present study shows that the surface temperature and coefficient of heat transfer can be reduced due to the effect of Re or $w\%$. For different $w\%$, it has been found that in the rise in the values of Re causes the increase of vortex length and as a result velocity gradient and $\triangle p$ arises. Furthermore, it has also been studied that the enhancement of Re causes the increase of P_p and $\triangle p$.

Keywords: Sudden expansion channel; Laminar flow; Heat transfer; Pumping power; Thermal enhancement factor.

*Corresponding Author email:v.ramachandraprasad@vit.ac.in

1 Introduction

At present time, researchers round the world are making considerable efforts to provide more effective heat transfer (HT) equipment in many industrial applications such as space and en-

ergy technology, electronic, aviation, medical applications. One of the active fields of research is to develop new methods and correct existing ones in order to improve the transfer rate of heat in tools and industrial technology. Due to less HT efficiency, the earlier HT applications are no longer active at present. To improve the cooling fluid thermal conductivity, many researchers [Bardenhagen et al. (2014); Karimipour et al. (2013); Moshizi et al. (2014)] have performed their work on different types of channels with the use of nanoparticles [Sunden et al. (2010); Karimipour et al. (2015)]. Moreover, to study the enhancement of HT capacity in cooling system, many researchers [Afrouzi et al. (2013); Sheikholeslami et al. (2016)] have investigated the usefulness of nanofluid instead of water. Furthermore, to increase the power generation in power plants, large number of authors presented that nanofluid is more useful rather than water [RamReddy et al. (2013); Akbari et al. (2016)]. Significant increase of convective HT coefficient without substantial loss of pressure becomes one of the considerable advantage causes for using nanoparticles. To reveal the thermo physical characteristics of nanofluids, many authors have considered different channel geometries such as backward and forward facing contracting channels [Alavi et al. (2015)], rectangular channel in presence of ribs [Sarlak et al. (2017); Toghraie et al. (2019)].

In a microchannel heat chamber, Peyghambarzadeh et al. (2014), experimentally studied the calm flow ofwater nanofluid/co_2 and H_2O-Al_2O_3. They have shown that in case of pressure profile, nanofluid becomes more pronounced than pure water. For the boundary conditions of slip and no-slip, Raisi et al. (2011) numerically investigated the characteristics of thermal phenomenaof water nanofluid-copper oxide in a microchannel heat chamber. It has been shown in their work that the HT enhances with the increase of Re. In a microchannel along with wavy walls, Heidary et al. (2010) noted that the rate of HT is increased 50% in use of nanofluids as compared to water. In a rectangular geometry, Jung et al. (2009) also studied the different characteristics of HT of H_2O-Al_2O_3 nanofluid. They revealed that the HT rate would increase by about 32% for 1.8% volume fraction. Behnampour et al. (2017) numerically studied the HT properties of laminar water/AgO nanofluids through a rectangular micro-channel with different types of baffles. For $[0-4]\%$ volume fractions, they concluded that the velocity profile became more prominent with rectangular baffles than other baffles, but the triangular baffles played a major role in thermal augmentation. In a two-dimensional and three-dimensional micro-channel, Akbari (a, b) et al. (2016) numerically solved the HT phenomena of H_2O-Al_2O_3 nanofluid at different baffle heights. They revealed that the in-

crease in thermal conductivity is due to the increase of baffle height, and volume fraction of the nanoparticles.

Using constant thermal boundary condition, Karimipour et al. (2015) investigated the forced HT coefficient of H_2O/Ag nanofluid through a rectangular micro-channel in presence of rectangular baffle. They have shown that increase in the value of Nu_{avg} causes the increase of Re and volume fraction. In presence of different pitches, Gravndyan et al. (2017) numerically studied the flow phenomena and the characteristics of HT of Water/TiO_2 in a two-dimensional rectangular micro-channel geometry. In their work, it is observed that the increase of Reynolds number flow velocity profile becomes more pronounced and complicated. Moreover, Abu (2008) numerically investigated the laminar nanofluids flow through a backward facing channel for volume fraction $[0.05 - 0.2]\%$. Furthermore, using nanofluid, various numerical and experimental studies on HT through different types of geometries have been considered by many authors [Parsaiemehr et al. (2018); Li et al. (2016); Andreozzi et al. (2016)].

After going through the above literature survey, it has been found that nanofluid plays a crucial role in the cool industry for studying the different flow characteristics and HT phenomena. It has become more interesting to study the different HT characteristics and pumping power (P_p), when the nanofluid flows through micro-channel geometry. Another interest is to study the pressure drop and velocity profile with the variation of w, which is very much helpful in various industrial applications. The present study analyzes the different characteristics of nanofluid flow phenomena (velocity profile, pressure profile, and pressure drop ($\triangle p$)) and thermal behavior of water flow in presence or absence of carbon nanoparticles through a suddenly expanded channel for expansion ratio 3. In this study, different HT characteristics (static temperature profile, skin friction coefficient (C_f), friction factor (f), local Nusselt number ($Nu(x)$), average Nusselt number (Nu_{avg}), and pumping power) have been studied with respect to the variation of w, Reynolds number (Re), and Nusselt number (Nu).

2 Geometry configuration and dimensions

FLUENT software has been utilized to configure the geometry [fig. 1(a, b)] and simulation purpose. Flow is assumed to be viscous, two-dimensional, laminar, nanofluid, steady, Newtonian and incompressible. Inflow velocity (u_{in}), pressure outlet, no-slip and no-penetration

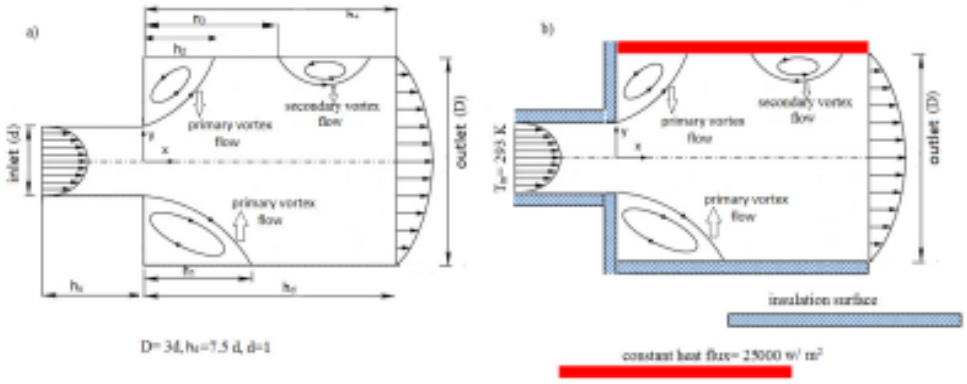

Figure 1: Schematic diagram of sudden expansion channel (a, b).

boundary conditions have been imposed on the inlet, outlet, and wall sections. The effects of radiation are negligible. Table 1 describes the properties of nanofluid in accordance with Nikkhah et al. (2015).

3 Mathematical formulation

Newtonian nanofluid flow through micro-channel is governed by the following equation-1 (continuity), equation-2 (x-momentum), equation-3 (y-momentum) and equation-4 (energy) [Raisi et al. (2014); Mahmoudi et al. (2012); Gholami et al. (2018)].

$$\frac{\partial u}{\partial x} + \frac{\partial v}{\partial y} = 0 \tag{1}$$

$$u\frac{\partial u}{\partial x} + v\frac{\partial u}{\partial y} = -\frac{\partial p}{\partial x} + \frac{\mu_{nf}}{\rho_{nf}\widehat{v_{nf}}}\frac{1}{Re}\left(\frac{\partial^2 u}{\partial x^2} + \frac{\partial^2 u}{\partial y^2}\right) \tag{2}$$

$$u\frac{\partial v}{\partial x} + v\frac{\partial v}{\partial y} = -\frac{\partial p}{\partial y} + \frac{\mu_{nf}}{\rho_{nf}\widehat{v_{nf}}}\frac{1}{Re}\left(\frac{\partial^2 v}{\partial x^2} + \frac{\partial^2 v}{\partial y^2}\right) \tag{3}$$

$$u\frac{\partial T}{\partial x} + v\frac{\partial T}{\partial y} = \frac{k_{nf}}{\rho_{nf}C_{nf}}\left(\frac{\partial^2 T}{\partial x^2} + \frac{\partial^2 T}{\partial y^2}\right) \tag{4}$$

Here, Re [Akbari (a) et al. (2016)], Nu [Sheikholeslami et al. (2016)], $\triangle p$ [Leng et al. (2015)], P_p and C_f [Leng et al. (2015)], R have been formulized as follows:

$$Re = \frac{\rho u_{in} d}{\mu} \tag{5}$$

$$Nu = \frac{hd}{k_f} \tag{6}$$

$$C_f = \frac{\tau_w}{2\rho u_{in}^2} \tag{7}$$

$$\triangle p = p_{out} - p_{in} \tag{8}$$

$$R = \frac{1}{h_d + h_u}\left(\frac{T_{max} - T_{in}}{25000}\right) \tag{9}$$

Whereas, ρ, μ, h, k, p_{out}, and p_{in} defined as density, dynamic viscosity, convective HT coefficient, thermal conductivity, pressure at outlet, pressure at inlet respectively.

3.1 Computational procedures, Grid independency test, and Validation of code

Ansys Fluent has been used for simulation and visualization purposes. Despite some compelling features of the finite volume method, the lower order interpolation of the convective terms in the governing equations causes several unwanted numerical effects. To avoid those, the QUICK scheme [Leonard's (1979)] has been utilized for spatial discretization of convective terms in the momentum equation. It is an upwind scheme that is accurate up to 3^{rd} order for the advection terms but 2^{nd} order for all other terms (diffusion terms). SIMPLEC algorithm [van Doormaal et al. (1984); Ternik et al. (2006)] resolves velocity and pressure coupling. As a result, using the SIMPLEC technique [van Doormaal et al. (1984); Ternik et al. (2006)], updated velocity and pressure fields satisfying exactly mass balance (the continuity equation) and essentially discrete momentum equations have been found. The detailed of the working procedure of SIMPLEC algorithm has been described in the introduction chapter. To study the effect of the mesh size, a grid test has been performed at $Re_n = 60$ as illustrated in the figures 2(a-b). The figures 2(a-b) represent the variation of pressure coefficients with the number of elements. Figure 2(b) stated that $91,220$ number of cells are enough for future analysis. Moreover, the figure 2(a) depicts a good remark between three different meshes (table 2). Furthermore, from the figure 2(a), it has been cleared that grid 2 can be taken for further analysis. Validation has been done with the studies of of Oliveira (2003) and Ternik et al. (2006) by analysis of primary vortex length (figure 3a) and normalized vortex length (figure 3b), which shows a good agreement [figures $3(a-b)$] of these with those of the present models. The configured geometry has been segregated into two different parts with the aid of fine mesh (figure 4).

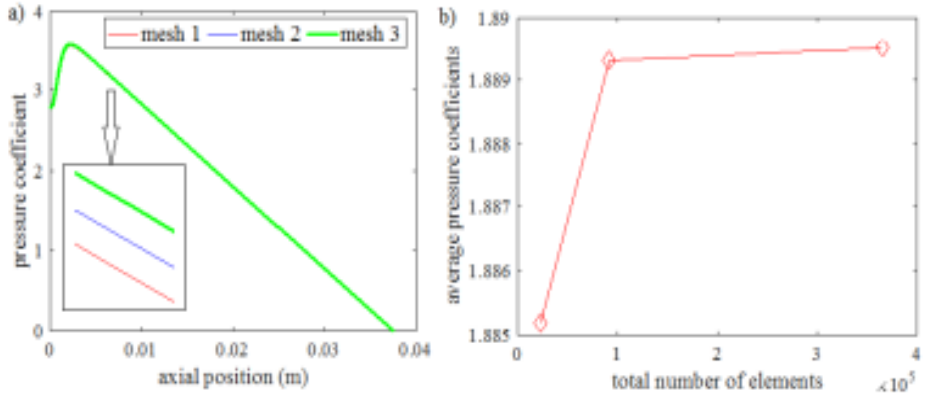

Figure 2: Plots of (a) pressure coefficients vs axial position and (b) average pressure coefficients vs total number of elements.

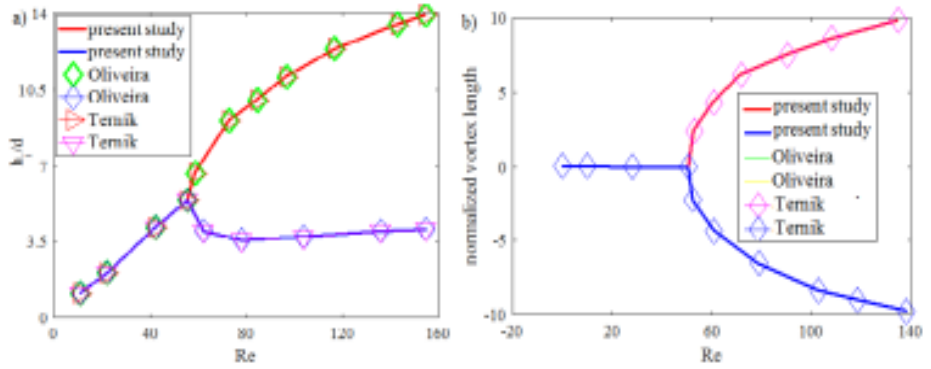

Figure 3: Plots of (a) length of primary vortex and (b) length of normalized vortex vs Re.

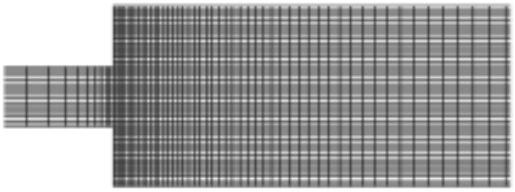

Figure 4: Mesh geometry.

Table 1: Nanofluid properties.

type	w	ρ (kg/m^3)	C_p	μ Pa-s	k_{nf}
pure water	0.00	995.8	4178	0.000765	0.62
water+CN	0.12	1003	4178	0.000780	0.65
water+CN	0.25	1008	4178	0.000795	0.68

Table 2: Grid study for pure water ($w\% = 0.00$).

grid	zone 1	zone 2	elements	average C_p
1	30×10	750×30	22910	1.8852
2	60×20	1500×60	91220	1.88930
3	120×40	3000×120	364840	1.889301

4 Results and discussions

4.1 Flow phenomena for $w\% = 0.00$

Figures 5 (a-c) and 6 (a-c) present the axial velocity and static temperature profiles for Re = 1, 50 and 130 respectively. Near the expanded section, it is found that the rate of non-viscous core penetration increases with the increase of inflow velocity (fig. 5). Moreover, it is observed that as the increase of Re, flow transition changes symmetric to asymmetric due to pressure drop and the flow moves to the outlet section of the channel. Furthermore,

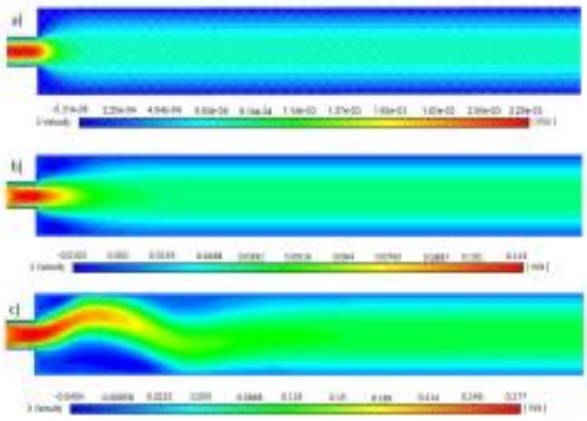

Figure 5: Axial velocity contour (a) Re = 1, 50 and (c) 130.

Figure 5 shows that low pressure zones are formed due to increase of flow velocity and pressure drop. In figure 6, it is demonstrated that the static temperature reduces as the inflow velocity increases. Because of the enhancement of cooling fluid momentum and the increase of Re, variation of temperature and kinetic energy reduces near the expanded section of the channel. Near the upper wall, it is found that an increase of Re causes the reduction of thermal boundary layer thickness (fig. 6). Furthermore, it has also studied that HT rate rises as Re increases.

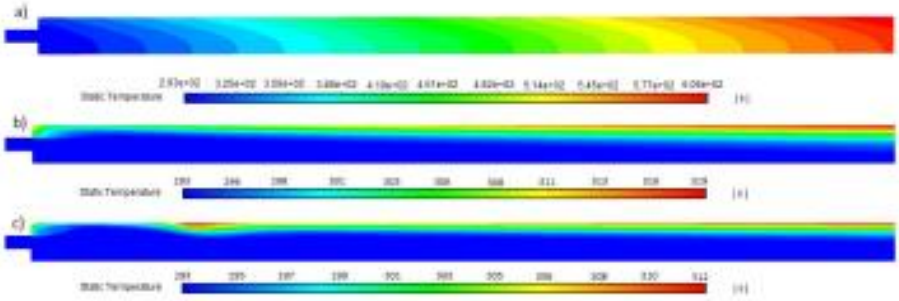

Figure 6: Static temperature profile at (a) $Re = 1$, 50 and (c) 130.

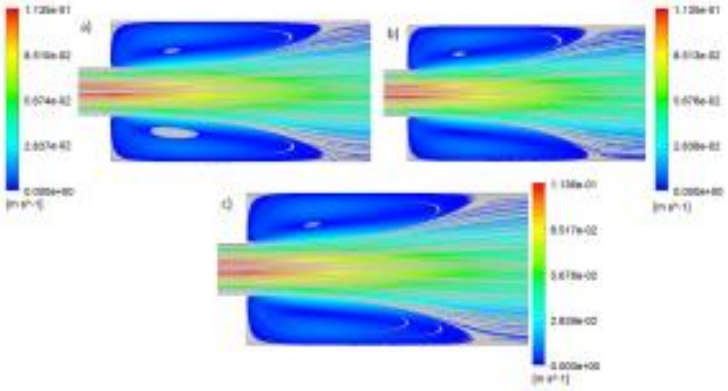

Figure 7: Velocity streamlines for (a) $w = 0$, (b) 0.12, and (c) 0.25 at $Re = 50$.

4.2 Effect of $w\%$

Figures 7 and 8 show the velocity streamlines for three various $w\%$, such as 0, 0.12, and 0.25 respectively. At $Re = 50$ (fig. 7), and $Re = 130$ (fig. 8) it is shown that the enhance of Re causes the enhancement of the length of vortex. From the color plot of figures 7(a-c) and 8(a-c), it is clearly observed that flow velocity increases as the weight percentage of nanoparticles increases. Figure 9 presents the bifurcation diagram for different weight percentage with respect to different values of Reynolds number. Moreover, for all the three taken weight percentages, it is found that the bifurcation of flow symmetry starts too break when $Re \leq 50$, which is shown in figures 7(a-c) and 9. It is found that different lengths of corner vortices exist when $Re > 50$. Further investigations revealed that $Re_{cr} = 49.8$ for weight percentage= 0.00, but for weight percentage= 0.12, Re_{cr} becomes 49.93 and also $Re_{cr} = 50$ for the weight percentage= 0.25, which are clearly shown in figure 9. Re_{cr} is the point of exchange of stability. Therefore, it is observed that the value of Re_{cr} increases with the increase of weight percentage. For different values of Re, pressure drop characteristics have been presented in figure 10. It is found that pressure drop gradually increases with the

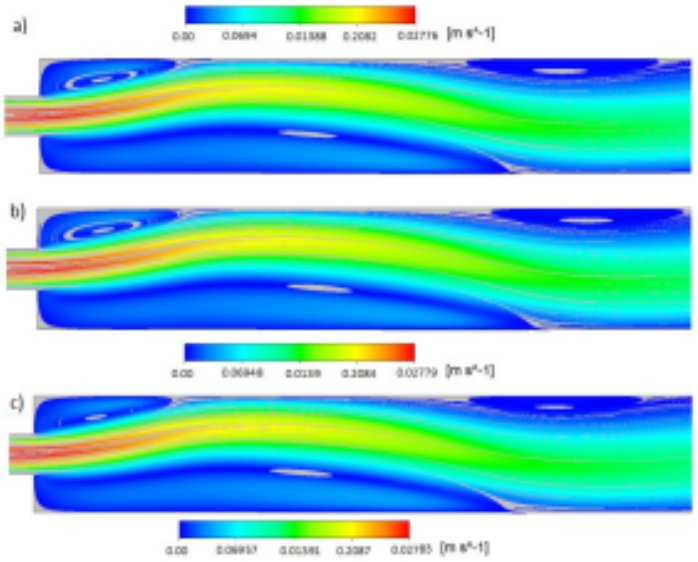

Figure 8: Velocity streamlines for (a) $w = 0$, (b) 0.12, and (c) 0.25 at $Re = 130$.

increase of Re. Moreover, for $w = 0.00, 0.12, 0.25$, it is observed that the pressure drop remains approximately the same at $Re = 1$. It has also been investigated that pressure drop becomes more pronounced at $w = 0.25$ rather than $w = 0.00$. As a consequence, these phenomena induce the decrease of momentum and an increase in pressure drop by enhancing the velocity of fluid in indirect paths.

4.3 Thermal behavior

For different Re, figure 12 (a-b) depicts the variation of skin friction coefficient and local Nusselt number along the upper wall for $w = 0.00$. Due to the presence of cross-sectional area and the variation of velocity on the channel, friction coefficient becomes more pronounced at higher values of Re [fig. 12(b)]. Moreover, it is also investigated that shear stress becomes higher as the axial velocity increases which causes the enhancement of friction coefficient. Along the hot channel wall, the variation of local Nusselt number has been presented in figure 12(a) for three weight percentages at different values of Re. At higher values of Re, it is studied that the profile of Nusselt number becomes more pronounced due to the increase of convective HT coefficient. As a result, rapid energy exchange of the cooling fluid causes an increase of HT rate. Moreover, it has also been studied that HT rate and Nu decreases at the beginning of the expanded section due to the increase rate of HT between fluid weight percentage and upper wall and decrease rate of thermal boundary layer. For various Re, the

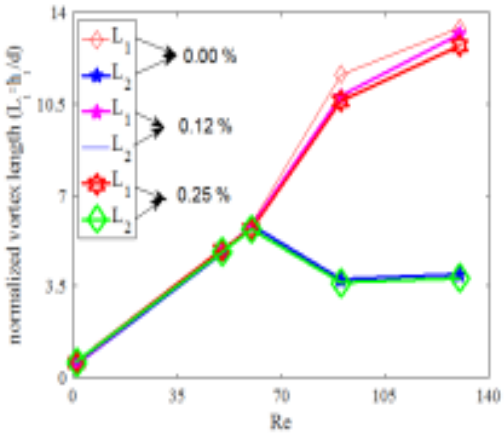

Figure 9: Bifurcation diagram for different weight percentages at different Re.

variation of friction factor has been shown in figure 13(a) for different values of w. As it is seen that, for all taken w, friction factor reduces as the increase of Re. Due to the decrease of boundary layer thickness and frictional effects the rate of flow reduces. Moreover, it is also observed that nanofluid particles interact with the wall surface for low values of Re. However, as the increase of Re, chances the interaction with the wall surface becomes higher. Furthermore, it is also observed that for sufficiently small values of w, there is an increase in the values of higher momentum at the upper wall. Figure 13(b) presents the profile of Nu_{avg} for different weight percentages at $Re = 1$, and $Re = 130$. Further study asserts that increase in the values of h and w cause the increase of Nu_{avg}. Figure 13(b) shows the linear relationship between Nu_{avg} and Re. For different values of Re, pumping power has been shown in figure 13(c) for three values of w. Strong pumps are required to achieve an adequate fluid velocity. Moreover, for all values of Re, it is investigated that pumping power increases with the increase of w due to the presence of nanoparticles in the cooling fluid. Furthermore, it is studied that a high rate of pumping power is required for $w = 0.25$ (high density and high viscosity of fluid) as compared to $w = 0.00$. For three different w, the profile of thermal resistance factor has been shown in figure 11, at three different values of Re. R can be described as the efficient parameter to calculate the amount of thermal resistance. It is observed that the improvement of HT causes the significant decrease of R with the increase of Re. Moreover, it is also found that the amount of R becomes more pronounced at $Re = 1$, as compared to $Re = 130$.

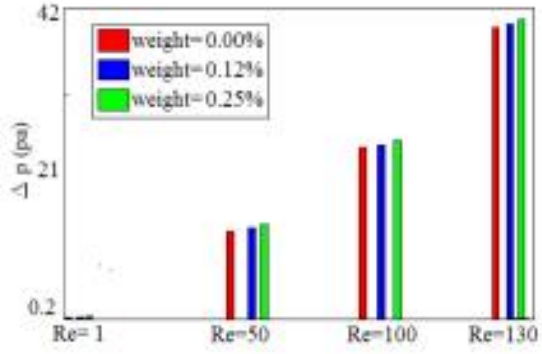

Figure 10: Pressure drop for various Re.

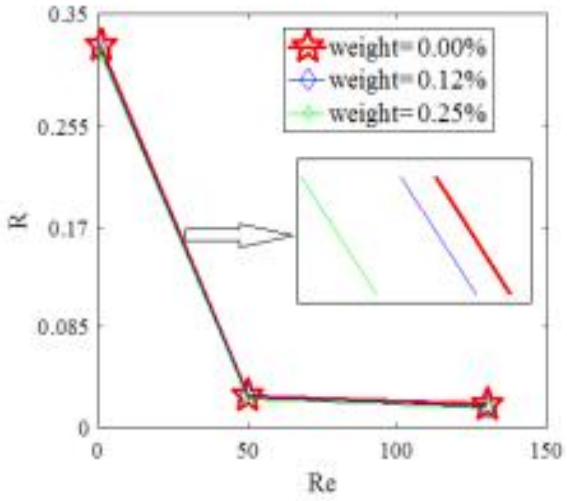

Figure 11: Thermal resistance factor vs Re.

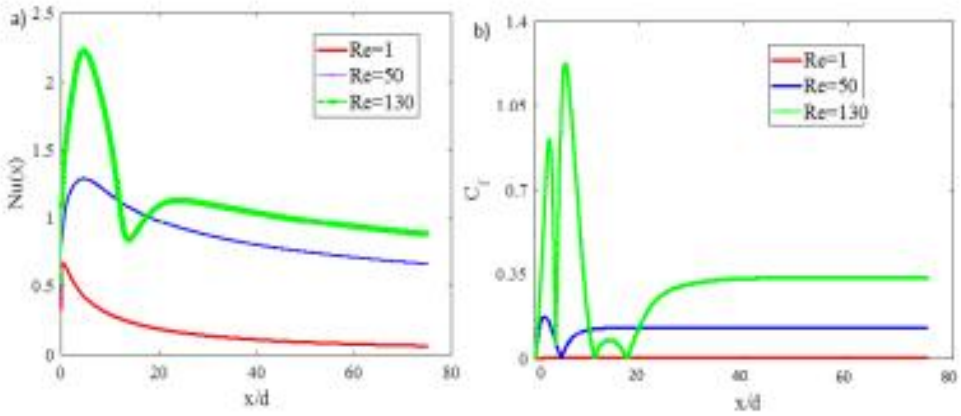

Figure 12: Plots of (a) $Nu(x)$ and (b) C_f at various Re.

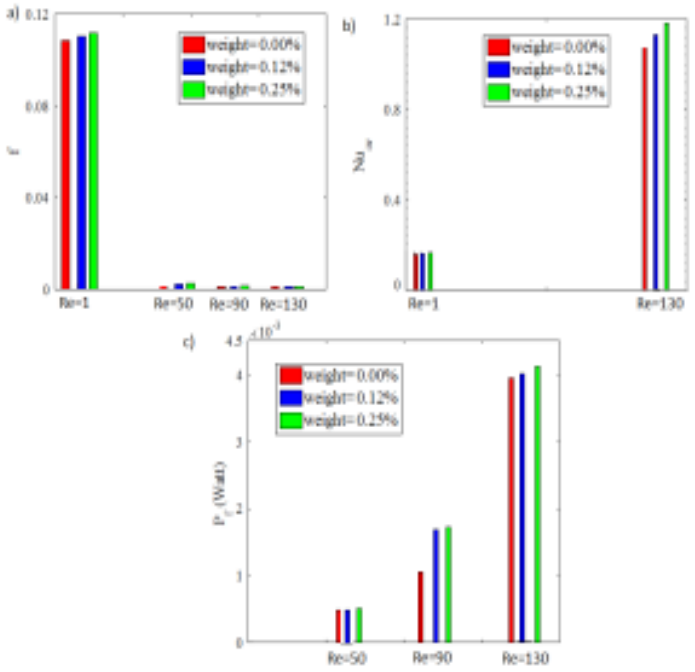

Figure 13: Plots of (a) f, (b) Nu_{avg}, and (c) P_p at various Re.

5 Conclusion

• It is observed with the increase of Re, flow transition changes symmetric to asymmetric. Moreover, for three different values of weight percentages, it has been revealed that two different lengths of corner vortices exist when $Re \leq 50$. But for $Re > 50$, flow bifurcation breaks the symmetry.

• It has been also investigated that $Re_{cr} = 49.8$ for $w = 0.00$, but for $w\% = 0.12$, Re_{cr} becomes 49.93 and also $Re_{cr} = 50$ for $w = 0.25$. Therefore, it is concluded that an increase of weight percentage causes the increase of Re_{cr}. It is also found that the increase of velocity causes the increase of friction coefficient, pressure drop as well as average Nusselt number. Moreover, it has also been noted that pressure drop becomes more enhanced at $w\% = 0.25$ as compared to $w\% = 0.00$.

• It is also observed that friction factor decreases with the increase of Re. In addition, it is concluded that an increase of Re causes the increase of Nu_{avg}. Pumping power increases with the increase of weight percentages and Re. Furthermore, it is also revealed that more pumping power is needed for $w\% = 0.25$ as compared to $w\% = 0.00$. Further investigation revealed that thermal resistance factor decreases with the increase of Re.

Conflict of interest

None

References

Abu, E. (2008). Application of nanofluids for heat transfer enhancement of separated flows encountered in a backward facing step, Int. J. Heat Fluid Flow, 29 (1), 242-249.

Akbari (a) O. A, Karimipour A, Toghraie D, Karimipour A (2016) Impact of ribs on flow parameters and laminar heat transfer of Water- aluminum oxide nanofluid with different nanoparticle volume fractions in a three- dimensional rectangular microchannel. Adv Mech Eng 7: 1-11.

Akbari (b) O. A, Toghraie D, Karimipour A (2016) Numerical simulation of heat transfer and turbulent flow of water nanofluids copper oxide in rectangular microchannel with semi attached rib. Adv. Mech. Eng 8(4): 1-25.

Alavi A, Safaei R. M, Mahian O, Goodarzi M, Dahari M, Yarmand Y, Wongwises H (2015) A hybrid finite element/finite difference scheme for solving the 3-d energy equation in transient non- isothermal fluid flow over a staggered tube bank. Numer. Heat Tran 68: 169-183.

Akbari (c) OA, Karimipour A, Toghraie D, Safaei R. M, Alipour G, Dahari M (2016) Investigation of Ribs height effect on heat transfer and flow parameters of laminar water- Al_2O_3 nanofluid in a two dimensional rib- microchannel. Appl Math Comp 290: 135- 153.

Afrouzi H. H, Farhadi M, Mehrizi A. A (2013) Numerical simulation of microparticles transport in a concentric annulus by Lattice Boltzmann Method. Adv. Powder Technol 24 (3): 575-584.

Andreozzi A, Manca O, Nardini S, Ricci D (2016) Forced convection enhancement in channels with transversal ribs and Nanofluids, Appl Therm Eng 98: 1044-1053.

Behnampour A, Akbarim O. A, Safaei M. R, Ghavami M, Marzban A, Shabani G. A. S, Zarringhalam M, Mashayekhi R (2017) Analysis of heat transfer and nanofluid fluid flow

in microchannels with trapezoidal, rectangular and triangular shaped ribs. Phys E 91: 15-31.

Bardenhagen K. A, Esfe M, Safaei M (2014) Mixed convection of copper-water nanofluid in a shallow inclined lid driven cavity using the lattice Boltzmann method. Physica A 402: 150-168.

Gravndyan Q, Akbari O. A, Toghraie D, Marzban A, Mashayekhi R, Pourfattah F (2017) The effect of aspect ratios of rib on the heat transfer and laminar water/TiO 2 nanofluid flow in a two dimensional rectangular microchannel. J Mol Liq 236: 254-265.

Gholami R. M, Akbari O. A, Marzban A, Toghraie D, Shabani G. A. S, Zarringhalam M (2018) The effect of rib shape on the behavior of laminar flow of oil/MWCNT nanofluid in a rectangular microchannel. Journal of Thermal Analysis and Calorimetry 134: 1611-1628.

Heidary H, Kermani M. J, (2010) Effect of nano- particles on forced convection in sinusoidal-wall channel. Int Commun Heat Mass 37: 1520-1527.

Jung J. Y, Oh H. S, Kwak H. Y, (2009) Forced convective heat transfer of nanofluids in microchannels. Int J Heat Mass Tran 52: 466-472.

Karimipour A, Nezhad A. H, Dorazio A, Ebrahim S (2013) The effects of inclination angle and Prandtl number on the mixed convection in the inclined lid driven cavity using lattice Boltzmann method. J Theor Appl Mech 51: 447-462.

Karimipour (b) A, Alipour H, Akbari O. A, Semiromi D. T, Esfe M. H (2015) Studying the effect of indentation on flow parameters and slow heat transfer of water-silver nano-fluid with varying volume fraction in a rectangular two-dimensional microchannel. Indian J Sci Technol 8(15): 1-13.

Khodabandeh E, Rahbari A, Rosen M. A, Ashrafi Z. N, Akbari O. A, Khodabandeh E, Abbasi A (2018) Performance optimization of water-Al2O3 nanofluid flow and heat transfer in trapezoidal cooling microchannel using constructal theory and two phase Eulerian-Lagrangian approach. Powder Technol 323: 103-114.

Leng C, Wang D. X, Wang H. T (2015) An improved design of double-layered microchannel heat sink with truncated top channels. Appl. Therm. Eng 79: 54-62.

Li Y. F, Xia G. D, Ma D. D, Jia Y. T, Wang J (2016) Characteristics of laminar flow and heat transfer in microchannel heat sink with triangular cavities and rectangular ribs. Int J Heat Mass Transf 98: 17-28.

Moshizi S. A, Malvandi A, Ganji D. D (2014) A two-phase theoretical study of Al2O3-water nanofluid flow inside a concentric pipe with heat generation/absorption. Int J Therm Sci 84: 347-357.

Moghiman M, Rahmanian B, Safaei R. M, Goodarzi M (2008) Numerical investigation of heat transfer in circular perforated plates exposed to parallel flow and suction. Int J Adv Des Manuf Technol 1(3): 43-56.

Mahmoudi H. A, Pop I, Shahi M (2012) Effect of magnetic field on natural convection in triangular enclosure filled with nanofluid. Int. J. Therm. Sci 59: 126-140.

Nikkhah N, Karimipour A, Safaei M. R, Forghani-Tehrani P, Goodarzi M, Dahari M, Wongwises S (2015) Forced convective heat transfer of water/functionalized multi-walled carbon nanotube nanofluids in a microchannel with oscillating heat flux and slip boundary condition. Int. Commun. Heat Mass Tran 68: 69-77.

Oliveira J. P (2003) Asymmetric flows of viscoelastic fluids in symmetric planar expansion geometries J. Non-Newtonian Fluid Mech 114: 33-63.

Parsaiemehr M, Pourfattah F, Akbari O. A, Toghraie D, Sheikhzadeh G. H, (2018) Turbulent flow and heat transfer of water/Al_2O_3 nanofluid inside a rectangular ribbed channel. Phys E 96: 73-84.

Peyghambarzadeh S. M, Hashemabadib S. H, Chabia R. A (2014) Performance of water based CuO and Al_2O_3 nanofluids in a Cube alloy heat sink with rectangular microchannels. Energ Convers Manage 86: 28-38.

RamReddy C, Murthy V. P, Chamkha J. A, Rashad A. M, (2013) Soret effect on mixed convection flow in a nanofluid under convective boundary condition. Int. J. Heat Mass Tran 64: 384-392.

Rezaei M, Azimian R. A, Toghraie D (2015) Molecular dynamics study of an electro-kinetic fluid transport in a charged nanochannel based on the role of the stern layer. Phys A Stat Mech Appl 426: 25-34.

Raisi A, Ghasemi B, Aminossadati M. S, (2011) A numerical study on the forced convection of laminar nanofluid in a microchannel with both slip and no-slip conditions. Numer Heat Tr A: Appl 59: 114- 129.

Safaei M. R, Rahmanian B, Goodarzi M (2011) Numerical study of laminar mixed convection heat transfer of power-law non- Newtonian fluids in square enclosures by finite volume method. Int J Phys Sci 6(33): 7456- 7470.

Sarlak R, Yousefzadeh S, Akbari O. A, Toghraie D, Sarlak S, Assadi F (2017) The investigation of simultaneous heat transfer of water/Al_2O_3 nanofluid in a close enclosure by applying homogeneous magnetic field. Int. J. Mech. Sci 133: 674-688.

Safaei MR, Goodarzi M, Mohammadi M (2011) Numerical modeling of turbulence mixed convection heat transfer in air filled enclosures by finite volume method. Int J Multiphys 5(4): 307-324.

Sunden B, Xie G (2010) Gas turbine blade tip heat transfer and cooling: a literature survey. Heat Transfer Eng 31: 527-554.

Sheikholeslami M, Gorji-Bandpy M, Ganji D. D (2016) Effect of discontinuous helical turbulators on heat transfer characteristics of double pipe water to air heat exchanger. Energy Convers Manag 118: 75-87.

Ternik P (2009) Planar sudden symmetric expansion flows and bifurcation phenomena of purely viscous shear-thinning fluids 157: 15- 25.

Toghraie D, Shirani E (2019) Numerical simulation of water/ alumina nanofluid mixed convection in square lid-driven cavity, Effect of magnetic field using a two-phase model. International Journal of Numerical Methods for Heat & Fluid Flow 30(5): 2782-2807.